

## Path-integral Monte Carlo study on a droplet of a dipolar Bose-Einstein condensate stabilized by quantum fluctuation

Hiroki Saito

*Department of Engineering Science, University of Electro-Communications, Tokyo 182-8585, Japan*

Motivated by the recent experiments [H. Kadau *et al.*, *Nature (London)* **530**, 194 (2016); I. Ferrier-Barbut *et al.*, arXiv:1601.03318] and theoretical prediction (F. Wächtler and L. Santos, arXiv:1601.04501), the ground state of a dysprosium Bose-Einstein condensate with strong dipole-dipole interaction is studied using the path-integral Monte Carlo method. It is shown that quantum fluctuation can stabilize the condensate against dipolar collapse.

Realization of Bose-Einstein condensates (BECs) of atoms with large dipole-dipole interaction (DDI)<sup>1–3</sup> has opened up the physics of ferromagnetic superfluidity. Experimental researches have been focused on the long-range and anisotropic nature of the DDI, such as anisotropic deformation<sup>4–6</sup> and excitation<sup>7,8</sup> of the cloud, anisotropic collapse and expansion,<sup>9,10</sup> and spinor-dipolar effects.<sup>11–13</sup>

Recently, the experimental group in Stuttgart observed<sup>14,15</sup> droplet lattice formation in a BEC of <sup>164</sup>Dy atoms, which have magnetic moment much larger than alkali atoms. A pancake-shaped BEC of <sup>164</sup>Dy atoms is prepared for a scattering length larger than the critical value for the dipolar collapse. The scattering length is then decreased to below the critical value for the collapse using Feshbach resonance, and the system becomes unstable due to the attractive part of the DDI. An instability, similar to the Rosensweig instability<sup>16,17</sup> in magnetic liquids, splits the condensate into droplets, and they form a stable triangular lattice.

Theoretical studies have been performed to explain the observation in the Stuttgart experiment. However, it has been found that simple mean-field theory, i.e., the Gross-Pitaevskii (GP) equation with DDI, cannot reproduce the experimental results; numerical studies of the GP equation have shown that the droplets always collapse immediately after they form, since the quantum pressure and *s*-wave repulsive interaction cannot support the attractive force of the DDI. To solve this problem, it was proposed that the droplets can be stabilized if large three-body repulsion exists. It was shown that the GP equation with appropriate strength of three-body repulsion can reproduce the experimental results.<sup>18,19</sup> Very recently, another mechanism to explain the stable droplets was proposed: Wächtler and Santos<sup>20</sup> showed that the GP equation with a Lee-Huang-Yang (LHY)<sup>21</sup> correction term can stabilize the droplets and reproduce the experimental results.

Motivated by the theoretical prediction in Ref. 20, in this Letter, we examine whether the quantum fluctuation can stabilize the droplet against dipolar collapse, using the path-integral Monte Carlo (PIMC) approach.<sup>22</sup> Many researchers have employed the PIMC method to explore the quantum

many-body properties of ultracold atoms.<sup>23–31</sup> We will show that a stable droplet state is obtained by the PIMC method, even when the ground state does not exist and the collapse occurs in the simple mean-field theory. The density profiles of the atomic clouds obtained by the PIMC method are compared with those by the GP equation with LHY correction proposed in Ref. 20.

We consider a system of <sup>164</sup>Dy atoms with mass *m* confined in a trap potential *V*(**r**), in which the direction of the magnetic dipole moment of the atoms is fixed to the *z* axis. The Hamiltonian for the system is given by

$$H = \sum_{j=1}^N \left[ \frac{\mathbf{p}_j^2}{2m} + V(\mathbf{r}_j) \right] + \sum_{j_1 < j_2} U(\mathbf{r}_{j_1} - \mathbf{r}_{j_2}), \quad (1)$$

where *N* is the number of atoms, and **r**<sub>*j*</sub> and **p**<sub>*j*</sub> are the position and momentum operators of the *j*th atom. The system is confined in a harmonic potential *V*(**r**) = *m*( $\omega_x^2 x^2 + \omega_y^2 y^2 + \omega_z^2 z^2$ )/2, where  $\omega_x$ ,  $\omega_y$ , and  $\omega_z$  are the trap frequencies. The interaction *U* between atoms consists of the hard-sphere potential with a radius *a* and the magnetic DDI as

$$U(\mathbf{r}) = U_{\text{hard}}(r) + \frac{\mu_0 \mu^2}{4\pi} \frac{1 - 3 \cos \chi}{r^3}, \quad (2)$$

where  $U_{\text{hard}}(r) = \infty$  for *r* < *a* and  $U_{\text{hard}}(r) = 0$  for *r* > *a*,  $\mu_0$  is the magnetic permeability of the vacuum,  $\mu = 9.93\mu_B$  is the magnetic dipole moment of a <sup>164</sup>Dy atom with  $\mu_B$  being the Bohr magneton, and  $\chi$  is the angle between **r** and the *z* axis. It is known that the *s*-wave scattering length coincides with the radius *a* of the hard-sphere potential.

In thermal equilibrium at temperature *T*, the probability that the atoms are located at  $R = \{\mathbf{r}_1, \mathbf{r}_2, \dots, \mathbf{r}_N\}$  is proportional to  $\sum_P \langle R | e^{-\beta H} | PR \rangle$ , where *P* represents permutation of indices to assure the Bose symmetry and  $\beta = 1/(k_B T)$  with  $k_B$  being the Boltzmann constant. The bracket  $\langle R | e^{-\beta H} | PR \rangle$  is divided into the path-integral form,

$$\int \dots \int dR_1 dR_2 \dots dR_{M-1} \langle R | e^{-\beta H/M} | R_1 \rangle$$

$$\times \langle R_1 | e^{-\beta H/M} | R_2 \rangle \cdots \langle R_{M-1} | e^{-\beta H/M} | PR \rangle, \quad (3)$$

where  $M$  is the number of ‘‘slices’’. Each bracket in Eq. (3) is approximated by

$$\langle R | e^{-\beta H/M} | R' \rangle \simeq P_{\text{noint}} P_{\text{hard}} P_{\text{ddi}}. \quad (4)$$

The part of noninteracting particles in a harmonic potential has the form,<sup>32</sup>

$$P_{\text{noint}}(R, R'; \tau) = \prod_{j=1}^N \prod_{\sigma=x,y,z} \left( \frac{m\omega_\sigma}{2\pi\hbar \sinh \omega_\sigma \tau} \right)^{1/2} \\ \times \exp \left\{ -\frac{m\omega_\sigma}{2\hbar \sinh \omega_\sigma \tau} \left[ (\sigma_j^2 + \sigma_j'^2) \cosh \omega_\sigma \tau - 2\sigma_j \sigma_j' \right] \right\}, \quad (5)$$

where  $\tau = \hbar\beta/M$ . For the hard-sphere interaction part in Eq. (4), we adopt the expression derived in Ref. 33,

$$P_{\text{hard}}(R, R'; \tau) \\ = \prod_{j_1 > j_2} \left\{ 1 - \frac{a(\rho_{12} + \rho'_{12} - a)}{\rho_{12}\rho'_{12}} \right. \\ \times \exp \left[ -\frac{1}{2\tau} (\rho_{12} - a)(\rho'_{12} - a) \left( 1 + \frac{\rho_{12} \cdot \rho'_{12}}{\rho_{12}\rho'_{12}} \right) \right] \\ \left. \times H(\rho_{12} - a) H(\rho'_{12} - a), \right. \quad (6)$$

where  $\rho_{12} = \mathbf{r}_{j_1} - \mathbf{r}_{j_2}$ ,  $\rho'_{12} = \mathbf{r}'_{j_1} - \mathbf{r}'_{j_2}$ , and  $H$  is the Heaviside step function, i.e.,  $P_{\text{hard}}$  vanishes when the distance between any two particles is less than  $a$ . The DDI part in Eq. (4) is approximated as

$$P_{\text{ddi}}(R, R'; \tau) \\ = \exp \left\{ -\frac{\tau \mu_0 \mu^2}{\hbar} \frac{1}{4\pi} \frac{1}{2} \sum_{j_1 < j_2} \left[ \frac{1 - 3 \cos \theta_{12}}{f_{\text{cutoff}}(\rho_{12})} + \frac{1 - 3 \cos \theta'_{12}}{f_{\text{cutoff}}(\rho'_{12})} \right] \right\}, \quad (7)$$

where  $f_{\text{cutoff}}(r) = r^3$  for  $r > R_{\text{cutoff}}$  and  $f_{\text{cutoff}}(r) = R_{\text{cutoff}}^3$  for  $r < R_{\text{cutoff}}$ . The cutoff radius  $R_{\text{cutoff}}$  is introduced to avoid the steep increase in the DDI potential near  $r = 0$ , which ruins the calculation. The validity of the cutoff will be discussed later. Using these expressions of  $P_{\text{noint}}$ ,  $P_{\text{hard}}$ , and  $P_{\text{ddi}}$ ,  $\sum_P \langle R | e^{-\beta H} | PR \rangle$  is evaluated by the multilevel Metropolis sampling,<sup>22</sup> where  $R_1, R_2, \dots, R_{M-1}$ , and  $R$  are sampled with an appropriate probability. Taking the average of  $R$ , one obtains the density distribution  $n(\mathbf{r})$  of the atomic cloud in thermal equilibrium. Typically, after  $10^3$ - $10^4$  Monte Carlo sweeps are performed to relax the system,  $10^3$ - $10^4$  samples are taken for the average.

Before showing the PIMC results, we briefly review the mean-field theory with the LHY correction proposed in Ref. 20. The LHY correction of the chemical potential in a

homogeneous dipolar BEC with density  $n$  is given by<sup>34</sup>

$$\Delta\mu(n) = \frac{32}{3\sqrt{\pi}} gn \sqrt{na^3} F(\epsilon_{dd}), \quad (8)$$

where  $g = 4\pi\hbar^2 a/m$ ,  $\epsilon_{dd} = \mu_0 \mu^2 / (3g)$ , and

$$F(\epsilon_{dd}) = \frac{1}{2} \int_0^\pi d\theta \sin \theta [1 + \epsilon_{dd}(3 \cos^2 \theta - 1)]^{5/2}. \quad (9)$$

The integral in Eq. (9) is taken for the range in which the integrand is real. Using the local density approximation, the LHY correction in Eq. (8) is incorporated into the GP equation, giving

$$i\hbar \frac{\partial \psi}{\partial t} = \left[ -\frac{\hbar^2}{2m} \nabla^2 + V + g|\psi|^2 \psi \right. \\ \left. + \frac{\mu_0 \mu^2}{4\pi} \int d\mathbf{r}' \frac{1 - 3 \cos \chi'}{|\mathbf{r} - \mathbf{r}'|^3} |\psi(\mathbf{r}')|^2 + \Delta\mu(|\psi|^2) \right] \psi, \quad (10)$$

where  $\chi'$  is the angle between  $\mathbf{r} - \mathbf{r}'$  and the  $z$  axis. The macroscopic wave function  $\psi$  is normalized as  $\int |\psi|^2 d\mathbf{r} = N$ . The DDI energy and the LHY correction  $\Delta\mu$  are roughly proportional to  $|\psi|^2$  and  $|\psi|^3$ , respectively. Therefore, when the peak density is increased by the DDI, the energy is dominated by the LHY correction term, which stops the collapse. The LHY quantum fluctuation can thus prevent the collapse and stabilize droplets. In the following results, the stationary states of the GP equation are obtained by the imaginary-time propagation method, in which  $i$  on the left-hand side is replaced with  $-1$  and the wave function is normalized in every time step.

We first check that the PIMC method reproduces the mean-field theory, when the LHY correction is small. We consider a system of  $N = 1024$  atoms confined in a harmonic trap with frequencies  $(\omega_x, \omega_y, \omega_z) = 2\pi \times (46, 44, 133)$  Hz.<sup>14</sup> We take  $\hbar\bar{\omega}\beta \equiv \hbar(\omega_x \omega_y \omega_z)^{1/3} \beta = 0.3$ , which corresponds to  $T \simeq 7.4$  nK. The critical temperature for Bose-Einstein condensation of an ideal Bose gas is  $T_c \simeq 0.94 \hbar\bar{\omega} N^{1/3} / k_B \simeq 29$  nK. Figure 1(a) shows the results without DDI, where  $a = 100a_0$  with  $a_0$  being the Bohr radius. We define the integrated density distributions as

$$n_x(x) = \frac{1}{N} \int n(\mathbf{r}) dy dz, \quad n_z(z) = \frac{1}{N} \int n(\mathbf{r}) dx dy, \quad (11)$$

where  $n(\mathbf{r})$  is the atom density. In Fig. 1(a), the density profiles obtained by the PIMC method almost agree with those by the GP equation. For these parameters, the GP results with and without the LHY correction cannot be discerned.

Figure 1(b) shows the result with DDI for  $a = 70a_0$ . For this value of  $a$ , the relative strength of the DDI is  $\epsilon_{dd} \simeq 1.87$  and the GP equation without the LHY correction has a metastable state, where the energy barrier originates from the quantum pressure.<sup>6</sup> Due to the anisotropic nature of the DDI, the atomic cloud is slightly elongated in the  $z$  direction and shrunk in the  $x$ - $y$  direction, compared with that without DDI. We see that the density distribution obtained by the PIMC

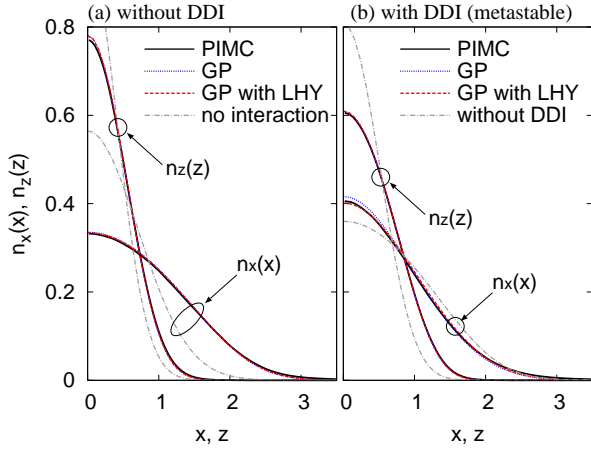


**Fig. 1.** Integrated density distributions  $n_x(x)$  and  $n_z(z)$  obtained by the path-integral Monte Carlo (PIMC) method (black solid curves) and the Gross-Pitaevskii (GP) equations without (blue dotted curves) and with (red dashed curves) the Lee-Huang-Yang (LHY) correction in Eq. (10).  $N = 1024$  atoms are confined in a harmonic potential with frequencies  $(\omega_x, \omega_y, \omega_z) = 2\pi \times (46, 44, 133)$ . (a) Density distributions without the dipole-dipole interaction (DDI), where  $a = 100a_0$  and  $M = 256$ . The gray dot-dashed curves show the harmonic oscillator ground state. (b) Density distributions of the metastable state with DDI, where  $a = 70a_0$ ,  $M = 256$ , and  $R_{\text{cutoff}} = 0.2a_x$ . For this value of  $a$ , the GP equation has a metastable state. The gray dot-dashed curves are obtained by the GP equation without DDI and LHY correction. The units of length and density distribution are  $a_x = [\hbar/(m\omega_x)]^{1/2}$  and  $a_x^{-1}$ .

method is in good agreement with those by the GP equation with DDI. This indicates that the PIMC method can be used to obtain not only the ground state but also a metastable state. The cutoff radius used in Fig. 1(b) is  $R_{\text{cutoff}} = 0.2a_x$ , where  $a_x = [\hbar/(m\omega_x)]^{1/2}$ . Almost the same result is obtained for  $R_{\text{cutoff}} = 0.1a_x$ .

We next examine whether the quantum fluctuation can stop the dipolar collapse. The state in Fig. 1(b) is the metastable state, and beyond the energy barrier, the energy of the atomic cloud decreases as it shrinks. If the LHY correction is absent, the GP equation has no lower energy bound and the peak density diverges; there is no ground state. The LHY correction in Eq. (10) suppresses the divergence of the peak density and allows the ground state.<sup>20</sup> To cross the energy barrier in the numerical calculations, the radial harmonic frequencies  $\omega_x$  and  $\omega_y$  are temporarily increased during Monte Carlo sweeps in the PIMC and during imaginary-time propagation in the GP equation, which shrinks the atomic cloud in the  $x$ - $y$  directions. Starting from these states, the system goes to the ground state beyond the energy barrier.

Figure 2 shows the density distributions of the state that has crossed the energy barrier, where the parameters are the same as those in Fig. 1(b). From Fig. 2(a), we find that both PIMC method and GP equation with LHY correction provide stable states, in which the dipolar collapse is suppressed and the peak density is kept finite. The density distribution obtained

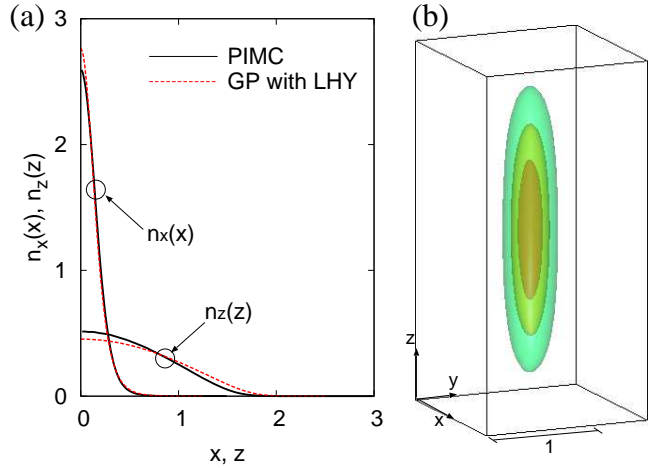


**Fig. 2.** (a) Integrated density distributions  $n_x(x)$  and  $n_z(z)$  obtained by the PIMC method (black solid curves) and the GP equation with LHY correction in Eq. (10) (red dashed curves). The parameters are the same as those in Fig. 1(b). There is no stable ground state in the GP equation without LHY correction for these parameters. (b) Isodensity surfaces obtained by the PIMC method. The surfaces represent 1/5, 2/5, and 3/5 of the peak density  $\approx 3 \times 10^{15} \text{ cm}^{-3}$ . The size of the frame is  $1.5 \times 1.5 \times 3$ . The units of length and density distribution are  $a_x = [\hbar/(m\omega_x)]^{1/2}$  and  $a_x^{-1}$ .

by the PIMC method slightly deviates from that by the GP equation with LHY correction, mainly due to the errors in the PIMC, which will be explained later. The GP equation with LHY correction may also be inaccurate due to the local density approximation. Figure 2(b) shows the isodensity surfaces of the three-dimensional density distribution obtained by the PIMC method. The atomic cloud is highly deformed to the cigar shape by the anisotropic DDI, while the trap potential is pancake shaped. The peak density in Fig. 2 is  $\sim 3 \times 10^{15} \text{ cm}^{-3}$  and the gas parameter is  $na^3 \sim 10^{-4}$ . The three-body recombination is expected to occur predominantly at the density peak, which is the reason for the atomic loss observed in the experiment.<sup>14</sup>

We check the validity of the cutoff made in the DDI potential in Eq. (7). Figure 3 shows the dependence of the density distribution  $n_x(x)$  on the cutoff radius  $R_{\text{cutoff}}$  and the number of slices  $M$  in the PIMC method. For  $R_{\text{cutoff}} = 0.25a_x$ , the distribution  $n_x(x)$  is substantially wider than others, and we presume that  $R_{\text{cutoff}} = 0.25a_x$  is too large to give the accurate result. For  $R_{\text{cutoff}} = 0.2a_x$ ,  $n_x(x)$  of the PIMC is close to that of the GP equation with LHY correction. Since the results of  $M = 256$  and  $M = 512$  are almost the same, the number of slices is enough. However, for  $R_{\text{cutoff}} = 0.15a_x$ ,  $n_x(x)$  significantly depends on  $M$ , when  $M$  is inadequate;  $M$  must be 2048 or larger. Therefore, the number of slices  $M$  must be increased with a decrease in  $R_{\text{cutoff}}$ . The computational amount is proportional to  $M$ , and the calculation for  $R_{\text{cutoff}} < 0.15a_x$  is extremely difficult. It seems that the density distribution converges to around that of the GP equation with LHY correction.

The accuracy of the present PIMC calculation is thus re-

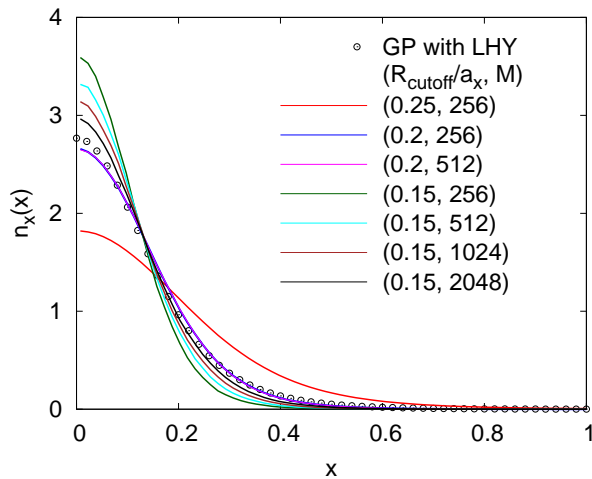


**Fig. 3.** Dependence of the density distribution  $n_x(x)$  on the cutoff radius  $R_{\text{cutoff}}$  and the number of slices  $M$  in the PIMC method. The value of  $a = 70a_0$  is the same as that in Fig. 2. From top to bottom of the peak values  $n_x(x = 0)$ ,  $(R_{\text{cutoff}}/a_x, M) = (0.15, 256)$ ,  $(0.15, 512)$ ,  $(0.15, 1024)$ ,  $(0.15, 2048)$ ,  $(0.2, 256)$ ,  $(0.2, 512)$ , and  $(0.25, 256)$ . The circles are obtained by the GP equation with LHY correction. The units of length and density distribution are  $a_x = [\hbar/(m\omega_x)]^{1/2}$  and  $a_x^{-1}$ .

stricted by the the primitive approximation of  $P_{\text{ddi}}$  in Eq. (7), whose  $r^{-3}$  steepness requires large numbers of slices  $M$  and Monte Carlo samplings. A more suitable expression for  $P_{\text{ddi}}$  is needed. Another bottleneck is the long-range nature of the DDI, which costs  $O(N^2)$  calculations per Monte Carlo sweep. The  $O(N)$  Monte Carlo technique<sup>35</sup> may circumvent this problem. With these improvements, it may be possible not only to perform more accurate calculation, but also to simulate the droplet pattern formation observed in the experiment with  $N \sim 10^5$  atoms.<sup>14</sup> The results obtained by the PIMC method should be compared with other methods, such as the diffusion Monte Carlo method.

In conclusion, we have investigated the stability of a strong dipolar BEC against collapse, motivated by the recent experiments<sup>14,15</sup> and the theoretical prediction.<sup>20</sup> Using the PIMC method, we showed that the system has a stable ground state even in the parameters for which the simple GP equation cannot sustain the system against dipolar collapse, which implies that the quantum fluctuation stabilizes the system. We compared the PIMC results with those obtained by the GP equation with the LHY correction proposed in Ref. 20, and found that they are in qualitative agreement. The present results indicate that the quantum fluctuation plays an important role in the droplet stabilization observed in the experiments.<sup>14,15</sup>

**Acknowledgments** I wish to thank Kui-Tian Xi for fruitful discussion. This work was supported by JSPS KAKENHI Grant Number 26400414 and by MEXT KAKENHI Grant Number 25103007.

- 1) A. Griesmaier, J. Werner, S. Hensler, J. Stuhler, and T. Pfau, Phys. Rev. Lett. **94**, 160401 (2005).
- 2) M. Lu, N. Q. Burdick, S. H. Youn, and B. L. Lev, Phys. Rev. Lett. **107**, 190401 (2011).
- 3) K. Aikawa, A. Frisch, M. Mark, S. Baier, A. Rietzler, R. Grimm, and F. Ferlaino, Phys. Rev. Lett. **108**, 210401 (2012).
- 4) J. Stuhler, A. Griesmaier, T. Koch, M. Fattori, T. Pfau, S. Giovanazzi, P. Pedri, and L. Santos, Phys. Rev. Lett. **95**, 150406 (2005).
- 5) T. Lahaye, T. Koch, B. Fröhlich, M. Fattori, J. Metz, A. Griesmaier, S. Giovanazzi, and T. Pfau, Nature (London) **448**, 672 (2007).
- 6) T. Koch, T. Lahaye, J. Metz, B. Fröhlich, A. Griesmaier, and T. Pfau, Nat. Phys. **4**, 218 (2008).
- 7) G. Bismut, B. Pasquiou, E. Maréchal, P. Pedri, L. Vernac, O. Gorceix, and B. Laburthe-Tolra, Phys. Rev. Lett. **105**, 040404 (2010).
- 8) G. Bismut, B. Laburthe-Tolra, E. Maréchal, P. Pedri, O. Gorceix, and L. Vernac, Phys. Rev. Lett. **109**, 155302 (2012).
- 9) T. Lahaye, J. Metz, B. Fröhlich, T. Koch, M. Meister, A. Griesmaier, T. Pfau, H. Saito, Y. Kawaguchi, and M. Ueda, Phys. Rev. Lett. **101**, 080401 (2008).
- 10) J. Metz, T. Lahaye, B. Fröhlich, A. Griesmaier, T. Pfau, H. Saito, Y. Kawaguchi, and M. Ueda, New J. Phys. **11**, 055032 (2011).
- 11) B. Pasquiou, E. Maréchal, G. Bismut, P. Pedri, L. Vernac, O. Gorceix, and B. Laburthe-Tolra, Phys. Rev. Lett. **106**, 255303 (2011).
- 12) B. Pasquiou, E. Maréchal, L. Vernac, O. Gorceix, and B. Laburthe-Tolra, Phys. Rev. Lett. **108**, 045307 (2012).
- 13) Y. Eto, H. Saito, and T. Hirano, Phys. Rev. Lett. **112**, 185301 (2014).
- 14) H. Kadau, M. Schmitt, M. Wenzel, C. Wink, T. Maier, I. Ferrier-Barbut, and T. Pfau, Nature (London) **530**, 194 (2016).
- 15) I. Ferrier-Barbut, H. Kadau, M. Schmitt, M. Wenzel, and T. Pfau, arXiv:1601.03318.
- 16) M. D. Cowley and R. E. Rosensweig, J. Fluid Mech. **30**, 671 (1967).
- 17) H. Saito, Y. Kawaguchi, and M. Ueda, Phys. Rev. Lett. **102**, 230403 (2009).
- 18) K. -T. Xi and H. Saito, Phys. Rev. A **93**, 011604(R) (2016).
- 19) R. N. Bisset and P. B. Blakie, Phys. Rev. A **92**, 061603(R) (2015).
- 20) F. Wächtler and L. Santos, arXiv:1601.04501.
- 21) T. D. Lee, K. Huang, and C. N. Yang, Phys. Rev. **106**, 1135 (1957).
- 22) D. M. Ceperley, Rev. Mod. Phys. **67**, 279 (1995).
- 23) W. Krauth, Phys. Rev. Lett. **77**, 3695 (1996).
- 24) P. Grüter, D. Ceperley, and F. Laloë, Phys. Rev. Lett. **79**, 3549 (1997).
- 25) M. Holzmann, W. Krauth, and M. Naraschewski, Phys. Rev. A **59**, 2956 (1999).
- 26) M. Holzmann and Y. Castin, Euro. Phys. J. D **7**, 425 (1999).
- 27) K. Nho and D. P. Landau, Phys. Rev. A **70**, 053614 (2004); *ibid.* **73**, 033606 (2006); *ibid.* **76**, 053610 (2007).
- 28) K. Nho and D. P. Landau, Phys. Rev. A **72**, 023615 (2005).
- 29) S. Pilati, K. Sakkos, J. Boronat, J. Casulleras, and S. Giorgini, Phys. Rev. A **74**, 043621 (2006).
- 30) M. Holzmann and W. Krauth, Phys. Rev. Lett. **100**, 190402 (2008).
- 31) A. Filinov, N. V. Prokof'ev, and M. Bonitz, Phys. Rev. Lett. **105**, 070401 (2010).
- 32) R. P. Feynman and A. R. Hibbs, *Quantum Mechanics and Path Integrals* (McGraw-Hill, New York, 1965).
- 33) J. Cao and B. J. Berne, J. Chem. Phys. **97**, 2382 (1992).
- 34) A. R. P. Lima and A. Pelster, Phys. Rev. A **84**, 041604(R) (2011); *ibid.* **86**, 063609 (2012).
- 35) K. Fukui and S. Todo, J. Comp. Phys. **228**, 2629 (2009).